CONF-801221--1

UCRL-84358
PREPRINT

MASTER

ACOUSTIC EMISSION UNDER BIAXIAL STRESSES IN UNFLAWED 21-6-9 AND 304 STAINLESS STEEL*

M. A. Hamstad
E. M. Leon
A. K. Mukherjee

For presentation at a conference on "Elastic Waves and Microstructures" at University of Oxford, England, December 16-17, 1980, and for publication in a special issue of Metal Science

October 31, 1980

Lawrence Livermore Laboratory

DISCLAIMER

Acoustic emission under biaxial stresses in unflawed 21-6-9 and 304 stainless steel*

M. A. Hamstad

University of California, Lawrence Livermore National Laboratory

Livermore, California 94550

E. M. Leon** and A. K. Mukherjee

University of California, Davis, California 95616

ABSTRACT

Acoustic emission (AE) testing has been carried out with uniaxial and biaxial (2:1 stress ratio) stressing of smooth samples of 21-6-9 and 304 stainless steel (SS). Uniaxial testing was done with simple tensile and compression samples as well as with the special biaxial specimens. Biaxial tensile stressing was accomplished with a specially designed specimen, which had been used previously to characterize AE in 7075 aluminum under biaxial stressing. Results were obtained for air-melt and for vacuum-melt samples of 21-6-9 SS. The air-melt samples contain considerably more inclusion particles than the vacuum-melt samples. For the 304 SS, "as received" material was examined. To allow AE correlations with microstructure, extensive characterization of the 21-6-9 microstructure was carried out. Significant differences in AE occur in biaxially stressed specimens as compared to uniaxially stressed samples.

---

*This work was performed under the auspices of the U.S. Department of Energy by the Lawrence Livermore National Laboratory under contract number W-7405-ENG-48.

**Present address: Hewlett Packard Corporation, Loveland, CO 80537

INTRODUCTION

Studies on characterizing the acoustic emission (AE) response of metals have gone on for at least 30 years. These studies have two major goals. The first goal is to use AE data to provide real-time information about the various deformation and microfailure mechanisms that occur when metals are stressed and deformed. The second goal is to characterize the AE generated in a particular metal alloy to allow us to better interpret the AE data obtained during flaw-location studies on structures made from this alloy.

Most of the AE characterization of smooth metal samples was done under simple uniaxial tensile loading of the test specimens. It was not until the mid-70's that the AE characterization of a metal alloy was done under uniaxial tension loading and then under uniaxial compression loading.[1-3] These results showed remarkable differences in the AE generated in 7075-T6 and in 7075-T651 aluminum under tensile and compressive loading. This and other information led to a more complete understanding of the AE sources operating in these materials.[4]

Recently, the first work was reported on the AE characterization of test specimens (taken from a single rod of 7075-T651) under biaxial tension (2:1 stress ratio) as well as under uniaxial-tension loading without a change in sample geometry.[5] These results showed AE generated in 7075-T651 under biaxial loading is of higher amplitude than that generated in the usual longitudinal tension test and is significant early in the macroscopically elastic region. On the other hand, AE generated in the longitudinal tensile test is not significant until macroscopic plastic deformation begins.

The purpose of this ongoing study is to extend to stainless steels (SS) the comparison of AE generated under uniaxial tension to AE generated under biaxial tension. This, and other extensions to common structural materials, is very important, because the vast majority of AE applications for flaw location in metal structures are under conditions of combined stress-loading. Hence, it is important to characterize AE sources from nonflawed samples under combined loading so that the higher amplitude and earlier AE, which has been shown in 7075-T651 under biaxial tension, is not mistaken for flaw growth.

SPECIMENS AND EXPERIMENTAL CONDITIONS

Two types of specimens were used: (1) a specially designed tubular specimen, which was loaded in tension or internally pressurized to produce biaxial tension (see Fig. 1); and (2) pin-type flat tensile samples (see Fig. 2). The smallest sample was used for transverse tensile samples. The reason for using the two types of specimens is primarily because of the cost savings possible by using the pin-type specimens. The work in Ref. 5 indicated that the two specimen types did not differ (except for a scale multiplier) in generating AE records under uniaxial tensile loading.

For the 21-6-9 material, tensile (Fig. 2a) and biaxial samples were aligned with the axial direction of the rod stock. In addition, some tensile samples were taken from the transverse direction (Fig. 2b). For the 304 SS material, the samples were taken from the rolling plane. Orientation with respect to the rolling axis was unknown.

The techniques discussed in Refs. 3 and 5 were tried in an attempt to eliminate and verify the level of extraneous AE noise. The techniques were successful for the biaxial test. They were not totally successful for uniaxial tension loading because interfacial stresses between the steel pins and the SS-specimen pin holes resulted in extraneous noise sources. To partially overcome this problem, we ran special AE tests to help distinguish real AE from extraneous AE during the tensile loading. These results will be developed later in this paper.

The 21-6-9 SS material was received in forged round-bar stock. The two 21-6-9 rods were produced by two manufacturing techniques: (1) air-melt and (2) vacuum arc remelt. Table 1 gives the chemical composition determined from a representative sample of each type of 21-6-9. Figures 3 and 4 show micrographs of three typical orthogonal views of the microstructure (grain size and shape, inclusion size and geometry) of a reduced section of a specimen. Because the two types of "as received" 21-6-9 SS had differing amounts of cold work, a common heat treatment was carried out to eliminate any differences. The steps in this heat treatment included (1) a vacuum anneal for one hour at 1010^{o}C; (2) a temperature drop to 650^{o}C in about one minute; and (3) a backfill of the furnace with argon to achieve the reduction to ambient room temperature.

The second alloy was 304 SS. This alloy was obtained in flat plate stock. Since these are preliminary tests prior to extensive testing with 304, no chemical or microstructural characterization was carried out.

The AE system consisted of (1) a piezoelectric, resonant-type AE transducer (Acoustic Emission Technology, Model C-175B for all tests except the transverse tensile samples which required a smaller sensor, Model MC-500), which is coupled to the gage section of the specimen by a viscous resin and held in place with a rubber band; (2) a preamplifier that gives a nominal electronic gain of 60 dB; (3) an amplifier and filter that gives an additional 20-to-40 dB electronic gain (bandpass set for 100 to 300 kHz); (4) an oscilloscope to monitor the AE signal; and (5) the AE data presentation system. The primary AE data recorded is the dc output from a root-mean-square (rms) voltmeter (Hewlett-Packard 3400A).

Tensile loads were applied in a standard tensile-testing machine at constant crosshead rates to yield a constant total strain rate in the plastic region. Internal pressurization was provided by a feedback control system that gave a constant total hoop-strain rate (about 0.2%/min) throughout the test. Clip gages were used to measure the axial and hoop strains and to provide a feedback signal for the constant-strain-rate pressurization tests. All tensile tests with the biaxial specimen were carried out with fluid in the specimen so that test conditions in the reduced section would be as near as possible (except for the stress field) to those in the internal pressurization tests.

ACOUSTIC EMISSION TESTS AND RESULTS

For the 21-6-9 material, we made tensile tests with both tensile samples and biaxial samples and made biaxial tests (2:1 stress ratio) with the biaxial samples. Figure 5 shows results for two air-melt samples under biaxial loading while Fig. 6 shows those typical of the biaxial specimen under uniaxial tensile loading. The corresponding data for the vacuum-melt specimens of the biaxial type are presented in Figs. 7 and 8. Figure 9 shows uniaxial tension results for transverse tension samples of both air- and vacuum-melt types. In tests for reloading the transverse tension samples (see Fig. 10), the sample was removed from the test machine and then reinstalled prior to reloading. For uniaxial tension results for longitudinal samples of the air- and vacuum-melt materials are given in Fig. 11.

Only a few tests with 304 SS were completed. Figures 12 and 13 show results typical of biaxial loading of the biaxial specimen and uniaxial tension of a pin-type tensile sample, respectively.

RESULTS AND DISCUSSION

From Figs. 5 and 6, as well as from 7 and 8, it is clear that when a smooth sample of 21-6-9 SS is subjected to a biaxial tension stress, the amplitude and amount of AE increases. Also there is considerable AE in the macroscopic elastic region for the biaxially loaded sample and little AE in the uniaxially loaded biaxial specimen for the same load region. These results are similar to earlier ones with 7075-T651 aluminum.[5]

Even though no 304 SS samples of the biaxial type were tested in uniaxial tension, the evidence suggests the same conclusions can be made for 304 SS as were made for 21-6-9 SS (see Figs. 12 and 13). The argument that a difference in specimen geometry could account for the difference between these figures can be overcome by the following fact. For both 7075-T651 aluminum and 21-6-9 SS, the essential quasi-continuous characteristics of the AE-rms results were the same in simple tension whether the biaxial specimen or the simple pin-type specimen was used (see Ref. 5 and Figs. 6, 8, and 11). In fact, the only apparent difference is one of relative amplitude of the quasi-continuous rms level. This is most easily explained by a volume difference between the two samples. The reduced section of the biaxial specimen is about 10 times larger in volume than that of the larger of the two pin-type samples in Fig. 2. Previous work[6] showed that the quasi-continuous rms level is expected to increase with the square root of the volume of the sample that is deformed.

Comparisons of Figs. 5 and 7, of Figs. 6 and 8, as well as of a and b of Fig. 9, indicate that the AE records for air-melt 21-6-9 SS differ significantly from those of the vacuum melt alloy for not only the biaxially loaded case but also for uniaxial tension of the transverse pin-type samples or the biaxial specimens of the two melts. It is necessary to discuss the melt AE differences for the short transverse samples in detail because of the grip noise problems indicated by the data in Fig. 10. Because of the small specimen size required to make transverse samples from existing materials, some compromises were required in the specimen design. The major compromise, the pin diameter, resulted in two separate sources of extraneous grip noise.

First, because the pins were not sufficiently strong to carry the loads, AE was generated by microcracking of the steel pins (tool steel). This conclusion was reached because rotating the pins 180^0 from the position in which they were previously loaded resulted in a maximum (as a function of angle of rotation) of extraneous burst-type AE. Also some new pins actually failed (with AE warning of impending failure) at loads below the maximum elastic load of the test specimens.

The second extraneous grip noise resulted from the bearing stresses of the steel pins against the pin hole in the SS sample. This problem was also a result of the size of the pin hole. As long as there was no change of relative position between mating surfaces between the first and second load cycles, the AE from this source was not detected during the second cycle. But, if the pin was moved by sliding it transverse to the load axis, extraneous AE noise was present during the second load cycle.

Because the extraneous AE was a random burst-type of insufficient number to change the relatively quasi-continuous rms levels, it was possible to use these levels in Fig. 9(a and b) to distinguish the air-melt samples from the vacuum-melt samples. As a function of strain, the rms peak for the air-melt sample typically was broader and occurred at a higher strain level, while the peak for the vacuum-melt sample was sharper and at a lower strain level.

The problem of the bearing stresses leading to random extraneous AE bursts was also present to a degree in the uniaxial tensile tests of the biaxial sample. This situation did not wholly result from higher bearing stresses than in the aluminum work,[5] where this extraneous noise was not a problem, but it seems to be because a steel-to-steel interface causes significantly more extraneous AE than does a steel-to-aluminum interface. We suggest the relative surface softness of 7075-T651 aluminum compared to stainless steel may mitigate the generation of AE by bearing stresses.

In the axial tensile data in Fig. 11(a and b), indications are that the same AE characteristics can be used to distinguish the air melt from the vacuum melt. The low AE signal level makes this difficult but does not necessarily imply that the transverse tension test is necessary to distinguish these two manufacturing processes when a simple pin-type sample is used. We conclude this because a different sensor was used for the transverse tensile tests. This AE transducer had a higher resonant frequency and a lower background electronic-noise level, which meant more gain could be used. Hence, the net effect may have been a more sensitive transducer for the transverse sample rather than a specimen-orientation effect.

Several other observations were made. First, under biaxial loading, the AE record is much more complicated for 21-6-9 than for 304 SS, which indicates more types of AE mechanisms and significant changes in these mechanisms with progressive deformation. Second, the vacuum-melt biaxial AE results are more consistent from sample to sample than the air-melt AE results (only one rod of each type material was used). This is expected since the vacuum melt process is more consistent. Third, the change in the 304 AE pattern from that observed under uniaxial loading is smaller than for the 21-6-9 AE pattern. Hence, it should be more straightforward to correlate the 304 AE data, rather than the 21-6-9 data, with microstructure. This thesis cannot yet be tested because a detailed microstructural study has only been carried out on the biaxially loaded 21-6-9 samples.

CORRELATION WITH MICROSTRUCTURAL RESULTS

The main differences between the air and vacuum melts of 21-6-9 were expected to relate to inclusions. Table 2 summarizes the results of a study of the inclusions in both types of samples. Micrographs of typical inclusions for the vacuum- and air-melt samples are shown in Figs. 14 and 15, respectively.

Before discussing the inclusion results, we must point out why we are not attempting to correlate the AE results with dislocation motion. First, when a compression test of the 304 SS was monitored, no AE was detected. Because AE had been detected in tension (see Fig. 13), we concluded that dislocation motion was not the source. Dislocation motion depends on shear stresses and thus is not dependent on whether the shear stresses are induced by external tension or by compression loading. Second, AE, which is associated with dislocation motion in commercial materials, is usually apparent at the onset of macroscopic yielding (see, for example, Ref. 7). In the current records, there are no AE peaks in the quasi-continuous rms level at this point in the stress-strain curves. Because the 21-6-9 data does not indicate any of this type of dislocation-based AE and because we expect compression tests of 21-6-9 to be similar to those of 304 SS, we assume that dislocation motion is not a significant contributor to the AE observed.

The distinctive characteristics of the 21-6-9 biaxial AE behavior are summarized in Table 3. Because of the complexities of the AE characteristics of 21-6-9 SS and because no single type of inclusion was present in both the air- and vacuum-melt samples, we will discuss only the main factors that must be reconciled in order to correlate the AE with the microstructural inclusions.

Hence, it appears likely that the burst-type AE must be associated with fracture and/or decohesion of large inclusion particles or of inclusion particles that release relatively large amounts of energy under these processes. In either case, the inclusions are not numerous. On the other hand, the quasi-continuous AE is associated with the same or other types of inclusions that are smaller in size or release less energy and, in either case, are orders of magnitude greater in number. For example, a Weibull distribution of inclusion sizes may lead to the observed results, i.e., a few large particles giving rise to burst type AE and many particles near the mean size giving rise to the quasi-continuous AE.

The level of the quasi-continuous AE in Fig. 5a (air melt No. 1) requires special discussion. This sample had a relatively high rms value, which increased from near yield to 1-1/2% strain before dropping very gradually. In contrast, air melt No. 3 (Fig. 5b) did not show this high level of quasi-continuous AE. The obvious difference between these two melts (Table 2) was the presence in air melt No. 1 of [Cr-Mn-O-Si]-rich (type C) inclusions, which showed extensive cracking. Possibly, if enough of these type C inclusions were present in the gage volume in air melt No. 1, they would raise the level of quasi-continuous emission to that observed in Fig. 5a.

Alternatively, one can also speculate on the possible occurrence of $M_{23}C_6$-type carbides that often form in the grain boundaries of 21-6-9 SS because of faulty heat treatment. These carbides by cracking or decohesion may contribute to the high level of quasi-continuous AE. Type $M_{23}C_6$ can be small enough to go undetected in optical metallography, the characterization technique employed in the present work. Another possibility suggested[8] is that short-range order, when present, can give rise to AE characteristics similar to those depicted in Fig. 5a. We are unaware at present of any x-ray or transmission electron microscope investigation to detect the presence of any ordering phenomenon in 21-6-9 steel.

The AE records of biaxially loaded vacuum-melt specimens (Fig. 7) are very irregular, showing the existence of two humps in the quasi-continuous AE record and a gradual rise in the rms value after approximately 2% strain. By optical metallography (Table 2), we detected only one type of inclusion (type D) and large variations in inclusion size. The larger inclusions had a tendency to be grouped together, whereas the smaller inclusions were more randomly dispersed. To reconcile the AE records with only one type of inclusion is difficult. The possibility exists that the observed AE results from cracking or decohesion (undetected by metallography) of a different type of inclusion or of one type of inclusion having two size distributions (e.g., bimodal or a more complicated distribution function).

One clear observation in the present series of tests is that burst-type AE is present in the biaxial tests whereas none or very little is observed in uniaxial tension. One is tempted to explain this in terms of an orientation effect, i.e., elongation of the inclusions in a specific direction (axial, in this case) with respect to the stress state (here, the presence of two-dimensional tensile stresses in the biaxial test). This could conceivably be the true explanation. However, this explanation is somewhat tempered by the fact that after allowing for differences of transducer sensitivity, strain rate, extraneous noise and specimen volume, the results depicted in Figs. 6

and 11a on one hand and Figs. 8 and 11b on the other hand are not all that dissimilar with respect to burst-type AE. If orientation of the inclusion with respect to stress-state were a major factor, we should have seen a bigger difference between AE records from longitudinal-tension and those from transverse-tension specimens.

CONCLUSIONS

1. Acoustic emission from 304 SS and 21-6-9 SS increases significantly under biaxial tensile loading compared to uniaxial tensile loading.
2. Acoustic emission from these materials seems to be primarily associated with inclusion contents.
3. For 21-6-9 SS, air melt can be distinguished from vacuum melt by the AE patterns.
4. As a function of strain under biaxial loading, AE from 21-6-9 SS is much more complicated than AE from 304 SS.
5. More research is required to specifically associate particular inclusions with the AE generated under biaxial and under uniaxial loading of stainless steel.

ACKNOWLEDGMENTS

The material was supplied by Dr. Clinton Heiple of Rockwell International. The authors thank R. G. Patterson and A. E. Brown for conducting the acoustic emission testing.

REFERENCES

1. M. A. Hamstad: "Continuous acoustic emission from 7075 aluminum," presented to 14th Acoustic Emission Working Group Meeting, San Antonio, Texas, 28-30 April 1975.

2. S. H. Carpenter: "Acoustic emission from plastic deformation," Proceedings of the ARPA/AFML Review of Quantitative NDE, AFML-TR-75-212, p. 643-665, 1976.

3. M. A. Hamstad and A. K. Mukherjee: A comparison of the acoustic emission generated by tensile and compressive testing of 7075 aluminum, Lawrence Livermore National Laboratory, Livermore, CA, Report UCRL-77502, 1975.

4. S. H. Carpenter and F. P. Higgins: "Sources of acoustic emission generated during the plastic deformation of 7075 aluminum alloy," Metall. Trans., 1977, 8A, 1629-1632.

5. M. A. Hamstad, R. G. Patterson, and A. K. Mukherjee: "Acoustic emission generated in unflawed 7075-T651 aluminum under uniform biaxial loading," Proceedings of 9th World Conference on Non-Destructive Testing, paper 4J-10, Melbourne, Australia, Nov. 1979.

6. M. A. Hamstad: On Energy Measurement of Continuous Acoustic Emission, Lawrence Livermore National Laboratory, Livermore, CA, Report UCRL-76286, 1974.

7. M. A. Hamstad, R. Bianchetti, and A. K. Mukherjee: "A correlation between acoustic emission and fracture toughness of 2124-T851 aluminum," Engineering Fracture Mechanics, 1977, 9, 663-674.

8. K. Ono, S.-Y. S. Hsu, K. Okajima, M. Yamamoto, and C. Ouchi: "Contributions to the Fifth Acoustic Emission Symposium," Technical Report No. 80-03 to Office of Naval Research, Contract No. N00014-75-C-0419, University of California, Los Angeles, Oct. 1980.

YDB:jp

LIST OF TABLES

Table 1 Chemical composition (wt%) of 21-6-9 stainless steel

Table 2 Inclusion characterization of 21-6-9 biaxially loaded specimens

Table 3 Acoustic emission characterization of 21-6-9 stainless steel biaxial tests

Table 1 Chemical composition (wt%) of 21-6-9 stainless steel

Element	Air-melt stock, 64-mm diam No. 1	Air-melt stock, 64-mm diam No. 3	Vacuum-melt stock, 51-mm diam
Cr	20.0	20.0	20.2
Ni	6.3	6.3	6.5
Mn	8.2	8.2	9.1
Si	0.22	0.22	0.45
Cu	0.2	0.2	0.2
Mo	0.2	0.2	0.06
Al	0.1	0.1	0.1
Co	0.1	0.1	0.1
Ca	0.01	0.01	0.01
Ag	0.001	0.001	0.001
Sr	0.0004	0.0004	0.0004
S	0.016	0.016	0.003
C	0.024	0.029	0.021
Ti	0.008	0.01	0.003
Nitrogen	0.353	0.350	0.299
Oxygen	0.013	0.018	0.009
P	0.030	0.019	0.013

Table 2 Inclusion characterization of 21-6-9 biaxially loaded specimens

Specimen	Type	Size	l/w[a]	Segregation tendency	Composition	Degree (%) of cracking	Color
Air melt No. 1	A	3-10 μm some larger	1:1	Found in stringers and globules	Mn,Cr,Ti,O	20-30%, mainly large inclusions	Dark gun-metal grey
	B	2-5 μm × 10-20 μm	4:1	Occasionally mixed with type A	Mn,S	No cracking	Grey-yellow tinge, lighter than A
	C	10-20 μm × 75-200 μm	10:1	Intermixed often; inclusions with other phases present	Cr,Mn,O,Si	300%[b], parallel to forging direction	Lighter than A or B
Air melt No. 3	A B	Characterization is the same as for No. 1 air melt.					
Vacuum melt Nos. 2 and 4	D	1-50 μm	1:1	No stringers but larger inclusions tended to group together, smaller ones randomly dispersed	Mn,Si,Mg,Cr,Ca,O	10%	About same color as type C

[a]Length to width ratio.

[b]300% implies 3 cracks per inclusion.

Table 3 Acoustic emission characterization of 21-6-9 stainless steel biaxial tests

Air melt No. 1	Air melt No. 3	Vacuum melt Nos. 2 and 4
i) High level of continuous AE	i) Lower level than No. 1 continuous AE	i) About the same as air melt No. 3
ii) Increase in continuous AE from yield up to about 1-1/2%, then falls off gradually with strain	ii) Peak in continuous AE just after yield, then falls off with strain	ii) Continuous AE starts to increase at about the 1-1/2 to 2% strain level and reaches a higher level than for air melt No. 3
iii) Substantial high-amplitude-burst AE	iii) Substantial high-amplitude-burst AE	iii) Fewer large amplitude bursts; total about 100
iv) Burst AE more intense before 2% strain	iv) Burst AE more intense before 2% strain	iv) Most burst AE occurs before 1 1/2% strain but not at as low a strain as in the air melts

List of Figures

Fig. 1. Drawing of AE biaxial-test specimen.

Fig. 2. Geometry of tensile samples.

Fig. 3. Micrographs showing grain structure (a) and inclusions (b) in three perpendicular planes taken from the reduced section of a biaxial specimen of vacuum-melt 21-6-9 SS (after a pressurization test).

Fig. 4. Micrographs showing grain structure (a) and inclusions (b) in three perpendicular planes taken from the reduced section of a biaxial specimen of air-melt 21-6-9 SS (after a pressurization test).

Fig. 5. Root-mean-square of AE and hoop stress shown as functions of hoop strain for biaxially tested 21-6-9 SS (gain 88 dB, background noise level 0.016 V). (a) Air melt No. 1. (b) Air melt No. 3.

Fig. 6. Root-mean-square of AE and axial stress shown as functions of axial strain for uniaxial test of biaxial specimen of 21-6-9 air melt (gain 88 dB, background noise level 0.020 V, strain rate in plastic region 0.02%/s).

Fig. 7. Root-mean-square of AE vs. hoop strain for biaxially tested samples of 21-6-9 vacuum melts 2 and 4 (gain 88 dB, background noise level 0.016 V).

Fig. 8. Root-mean-square of AE and axial stress vs. axial strain for uniaxial test of biaxial specimen of 21-6-9 vacuum melt (gain 88 dB, background noise level 0.020 V, strain rate 0.02%/s).

Fig. 9. Root-mean-square of AE and stress as functions of strain tension of 21-6-9 SS (gain 90 dB, background noise level 0.009 V, strain rate 0.25%/s). (a) Transverse vacuum-melt sample. (b) Transverse air-melt sample.

Fig. 10. Reload of samples from Fig. 9. (a) Sample from Fig. 9a. (b) Sample from Fig. 9b.

Fig. 11. Root-mean-square of AE and stress vs. strain for axial sample of 21-6-9 SS (gain 86 dB, background noise 0.015 V, strain rate 0.13%/)s. (a) Air-melt sample. (b) Vacuum-melt sample.

Fig. 12. Root-mean-square of AE and hoop stress vs. hoop strain for biaxial test of 304 SS (gain 88 dB, background noise 0.020 V).

Fig. 13. Root-mean-square of AE and stress vs. strain of tension of pin-type sample 304 SS (gain 88 dB, background noise 0.017 V, strain rate 0.20%/s).

Fig. 14. Typical type D inclusion in a vacuum-melt biaxial sample of a 21-6-9 SS.

Fig. 15. Typical type A, B, and C inclusions in an air-melt sample of 21-6-9 SS.

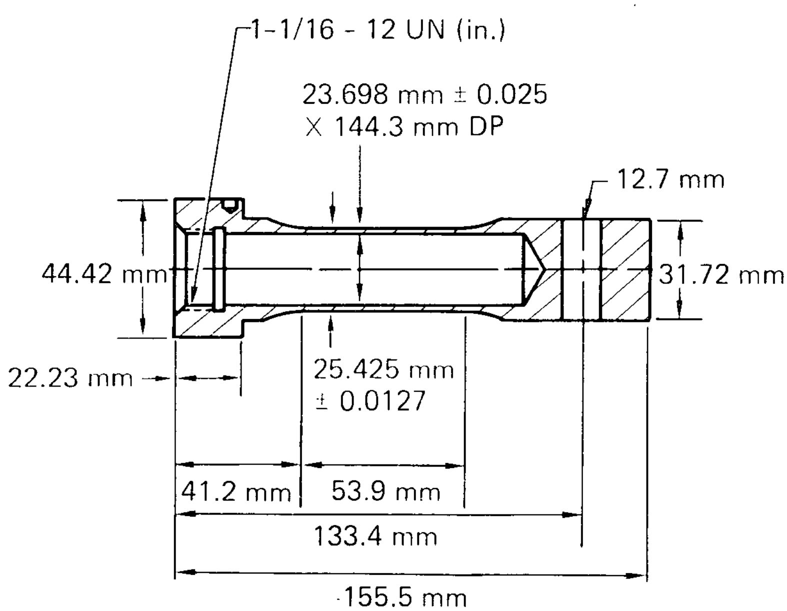

Fig. 1 - Hamstad

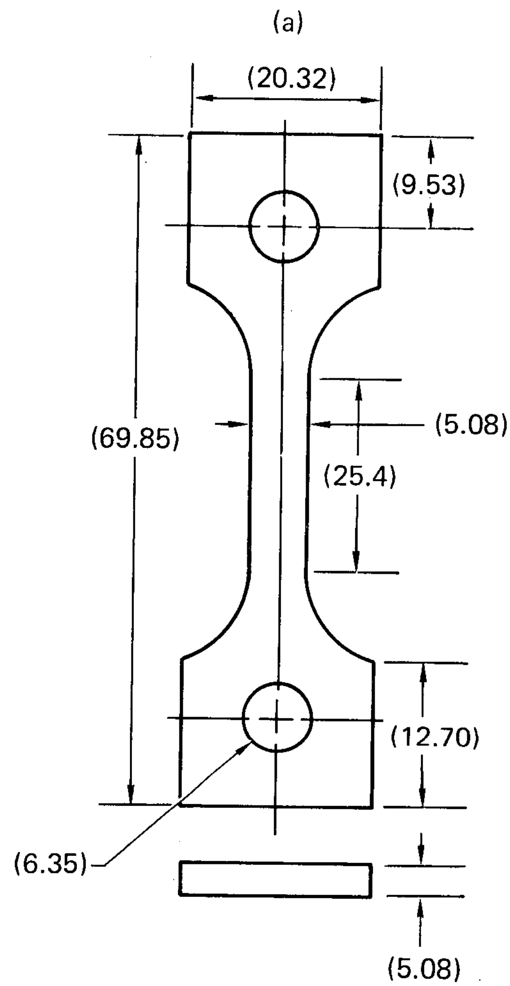

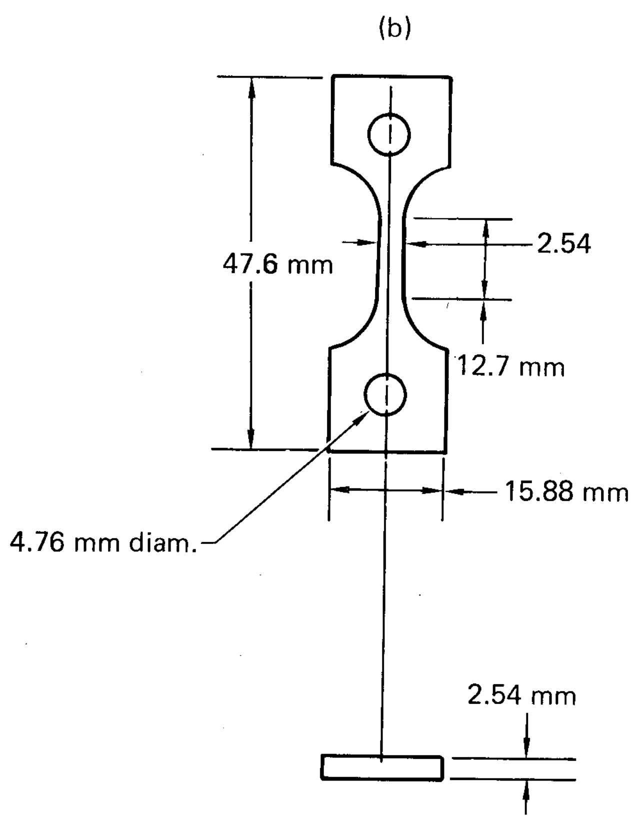

Fig. 2 - Hamstad

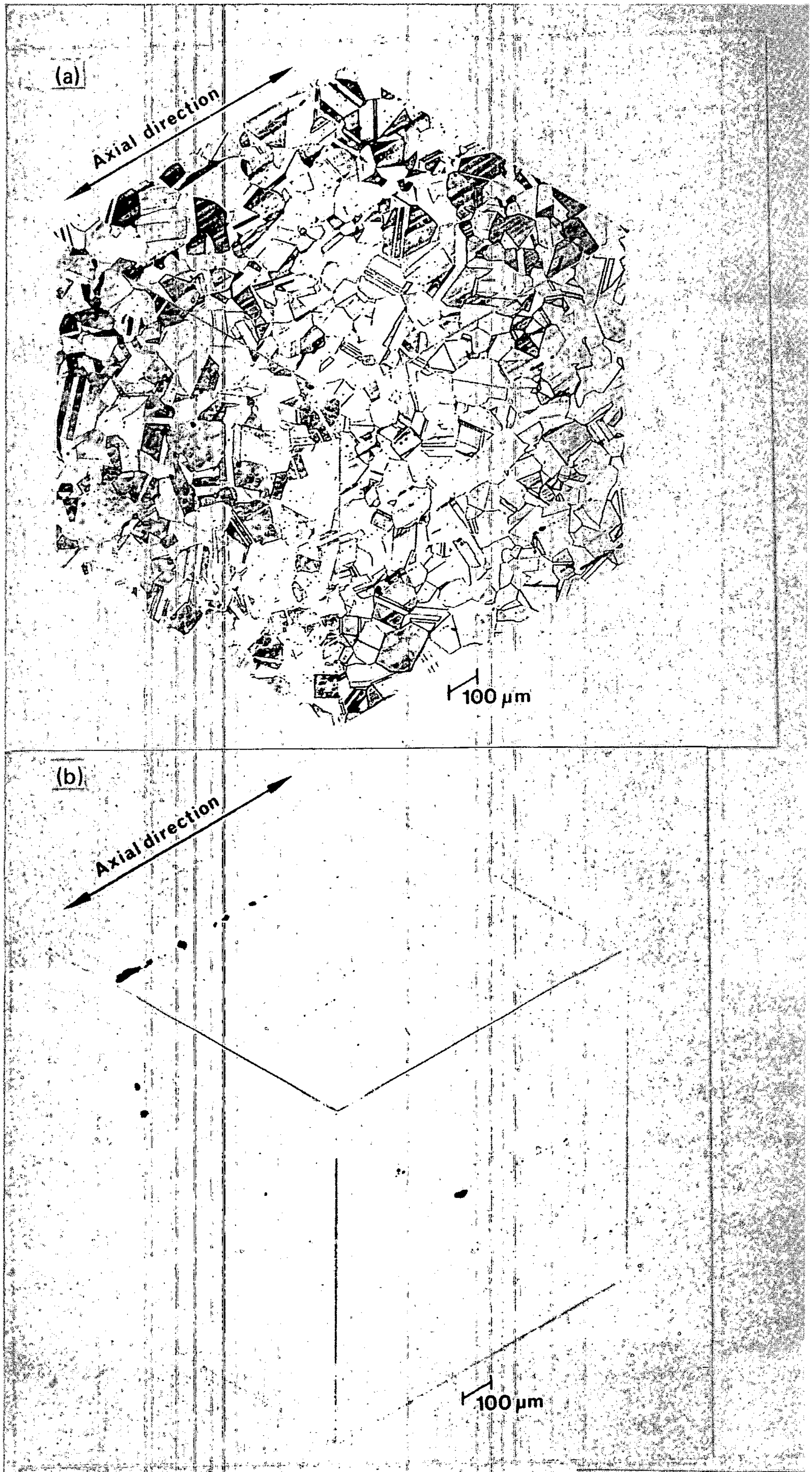

Fig. 3 - Hamstad

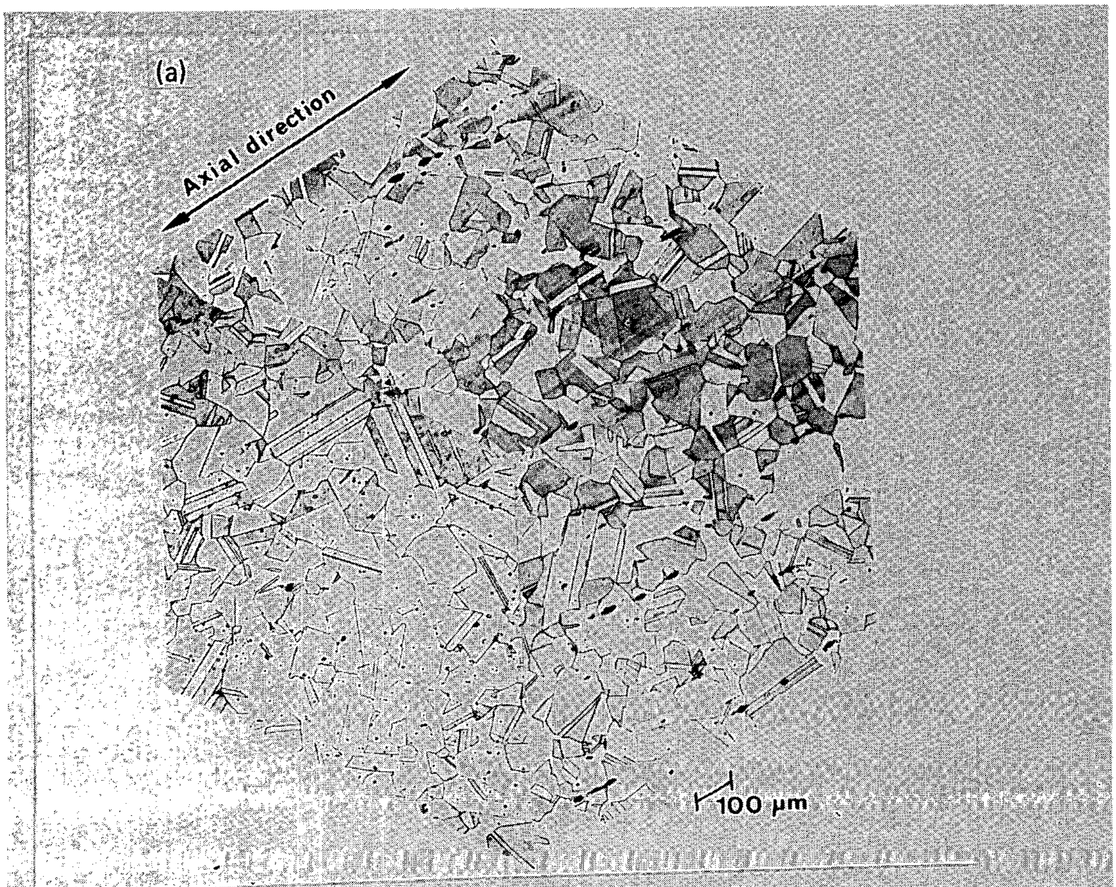

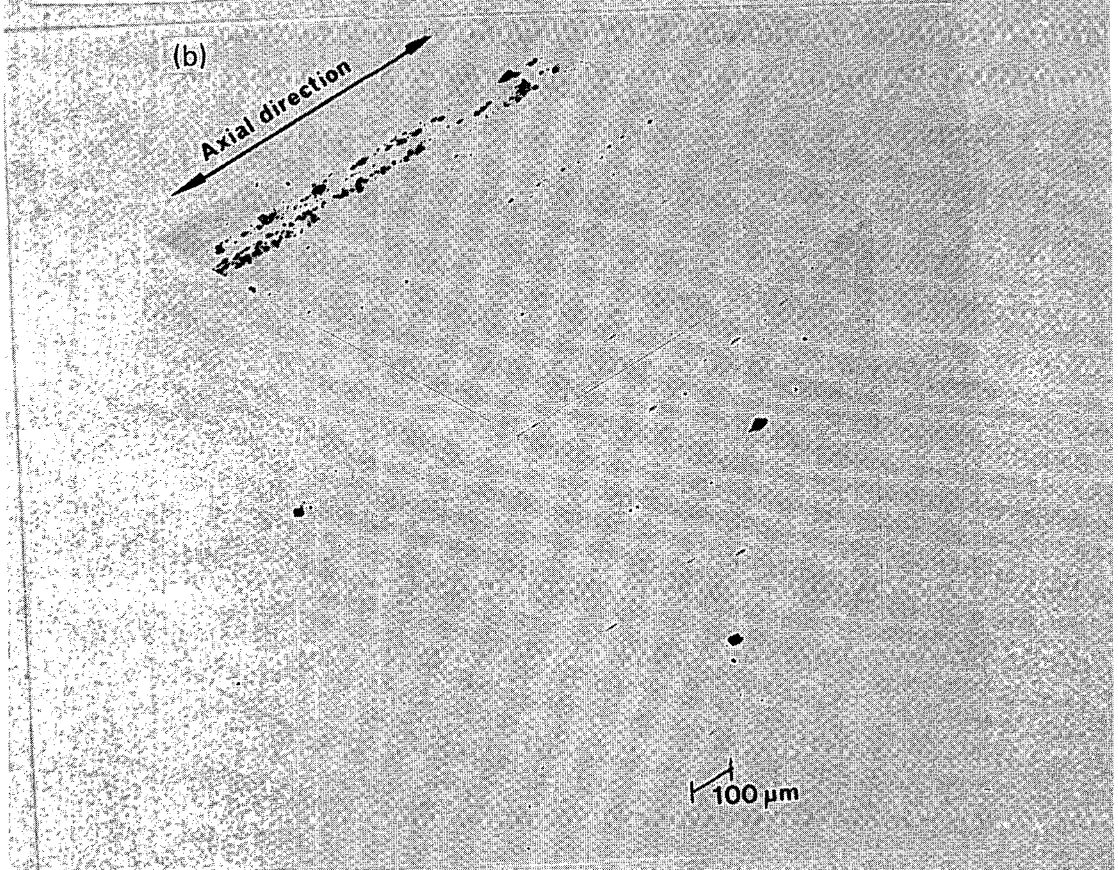

Fig. 4 - Hamstad

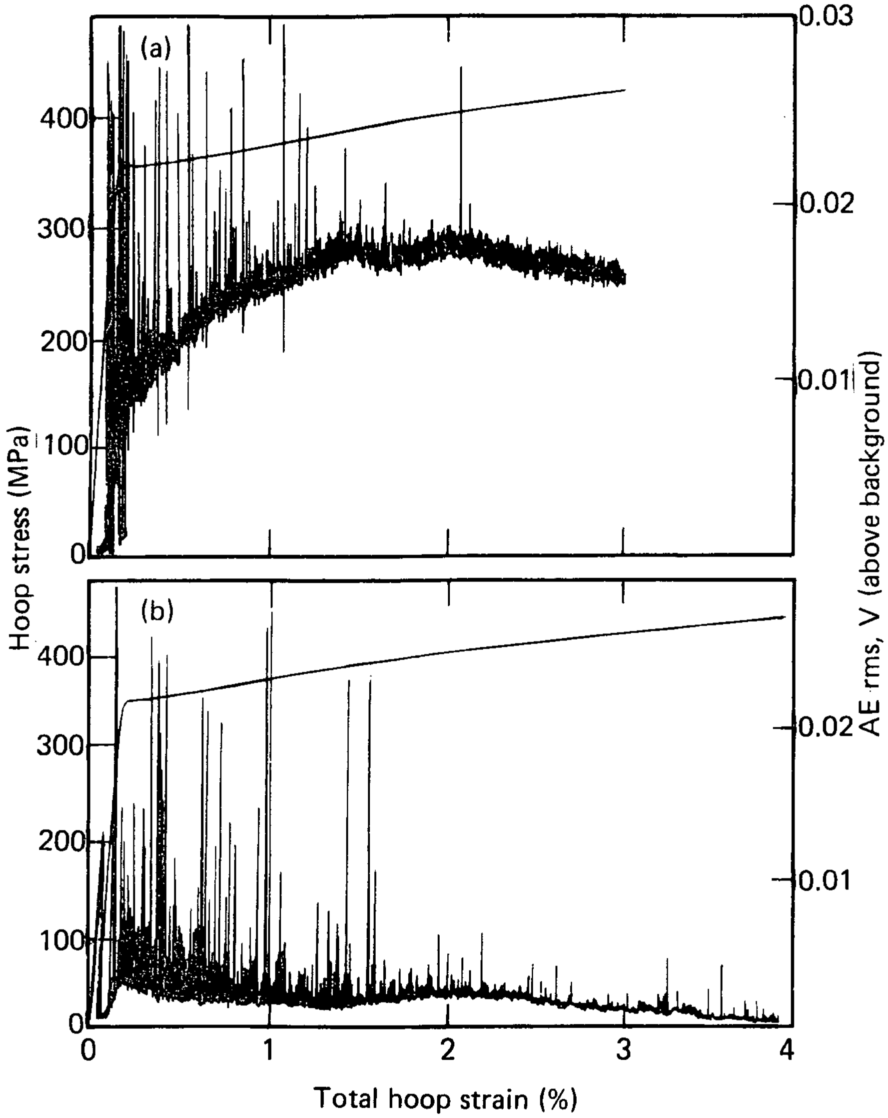

Fig. 5 - Hamstad

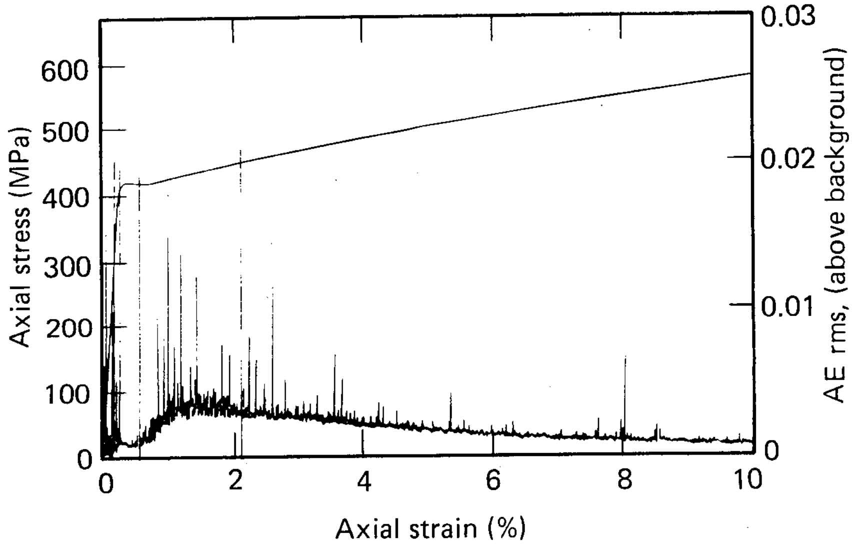

Fig. 6 - Hamstad

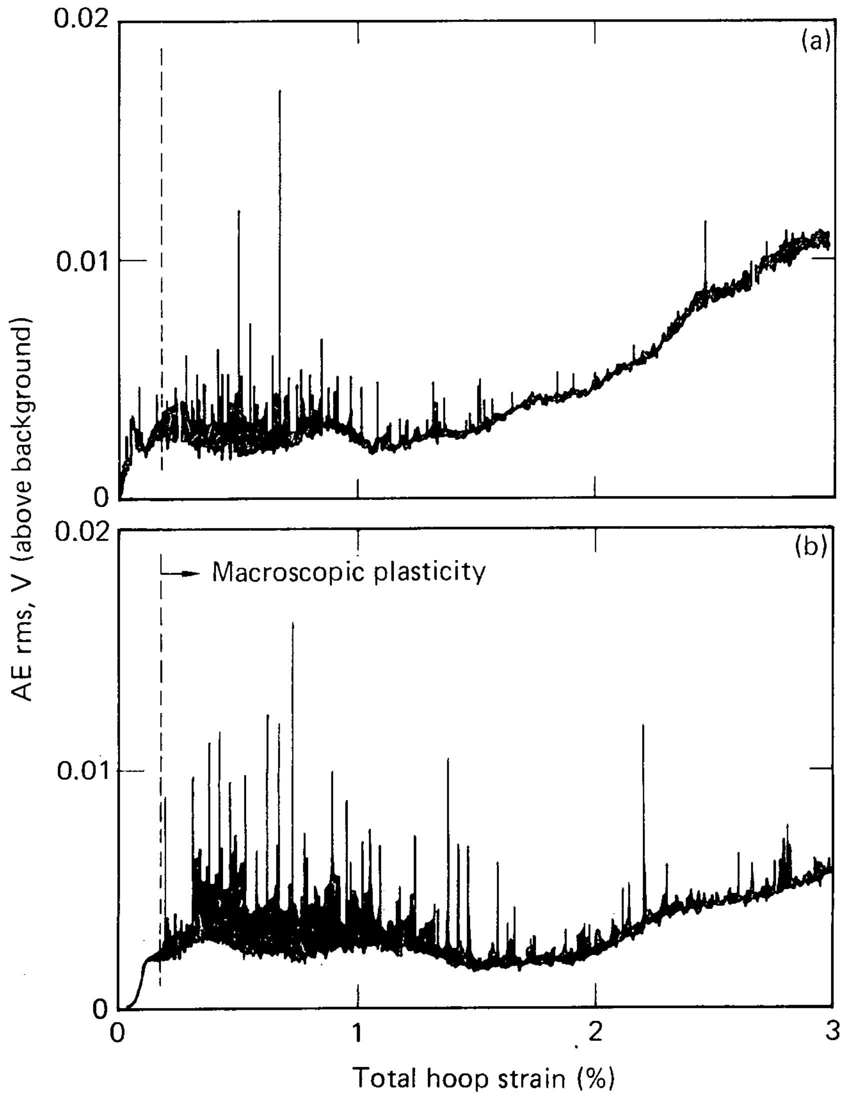

Fig. 7 - Hamstad

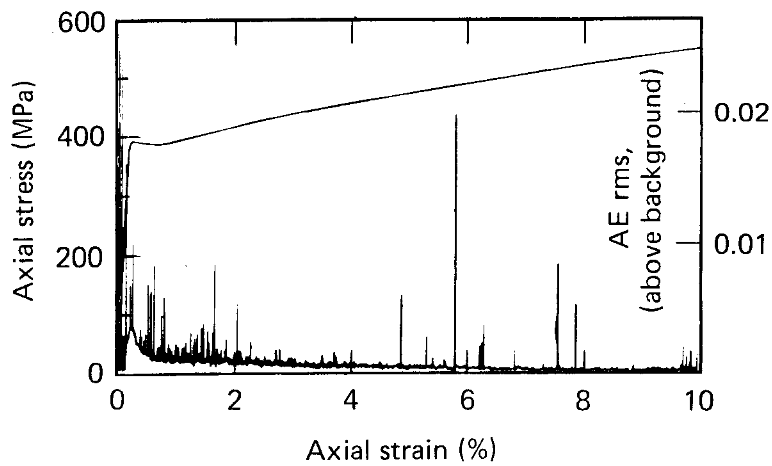

Fig. 8 - Hamstad

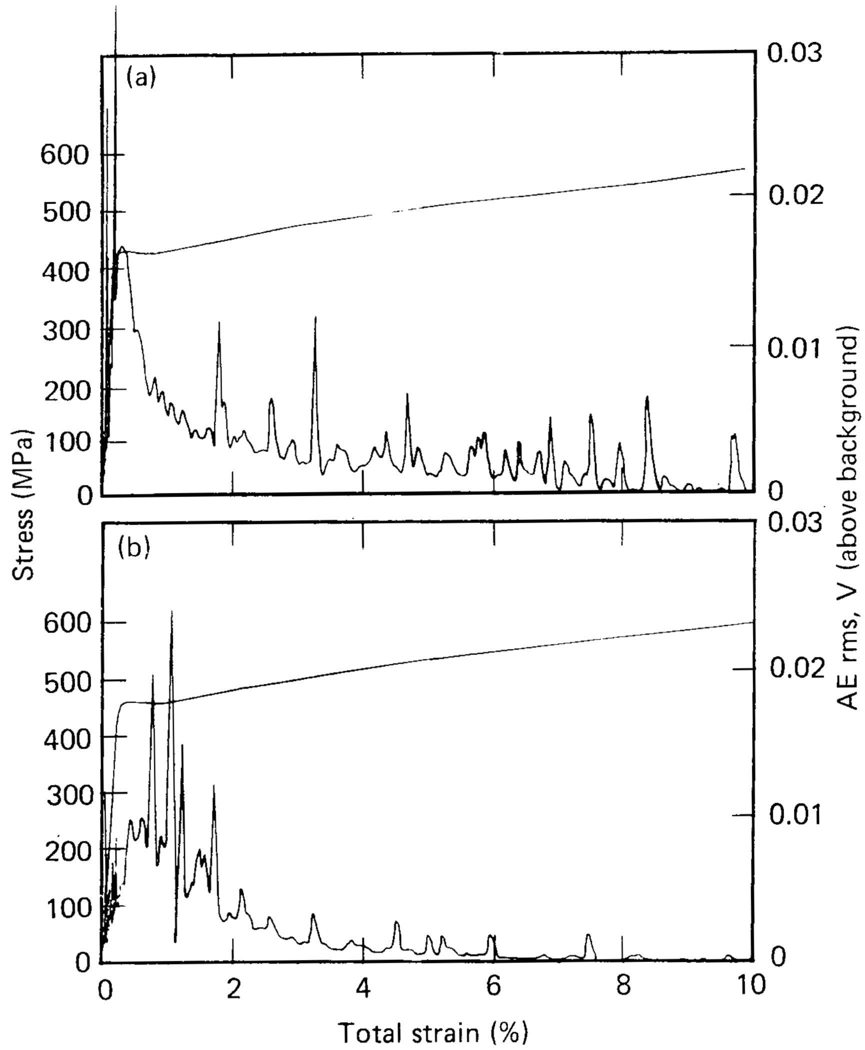

Fig. 9 - Hamstad

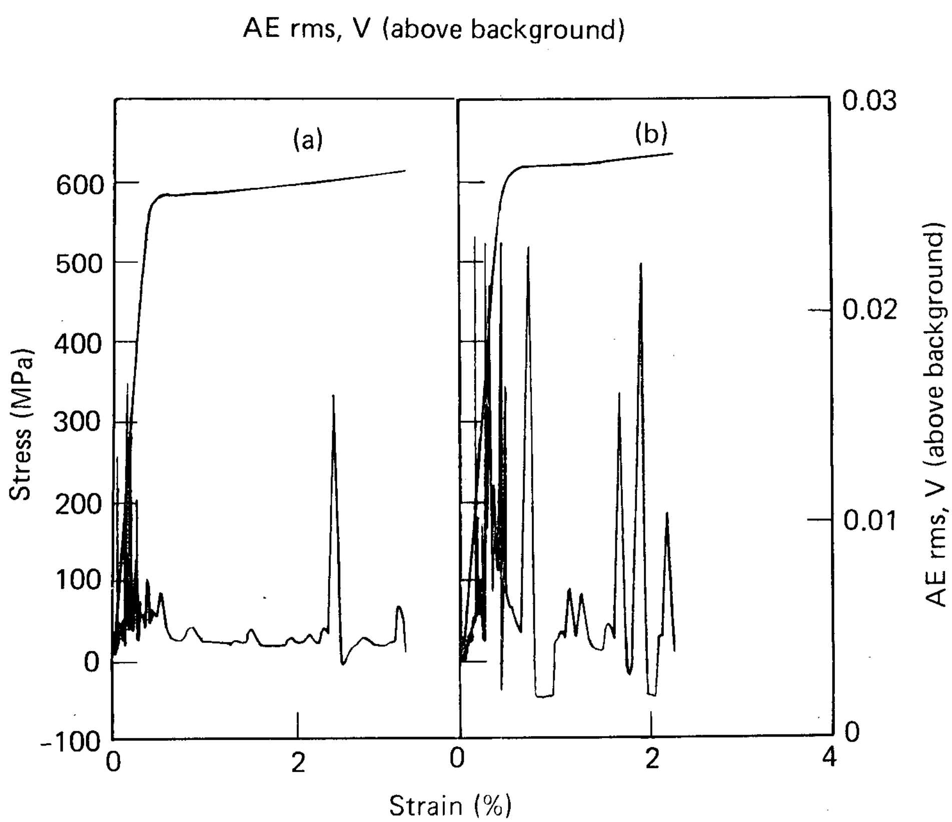

Fig. 10 - Hamstad

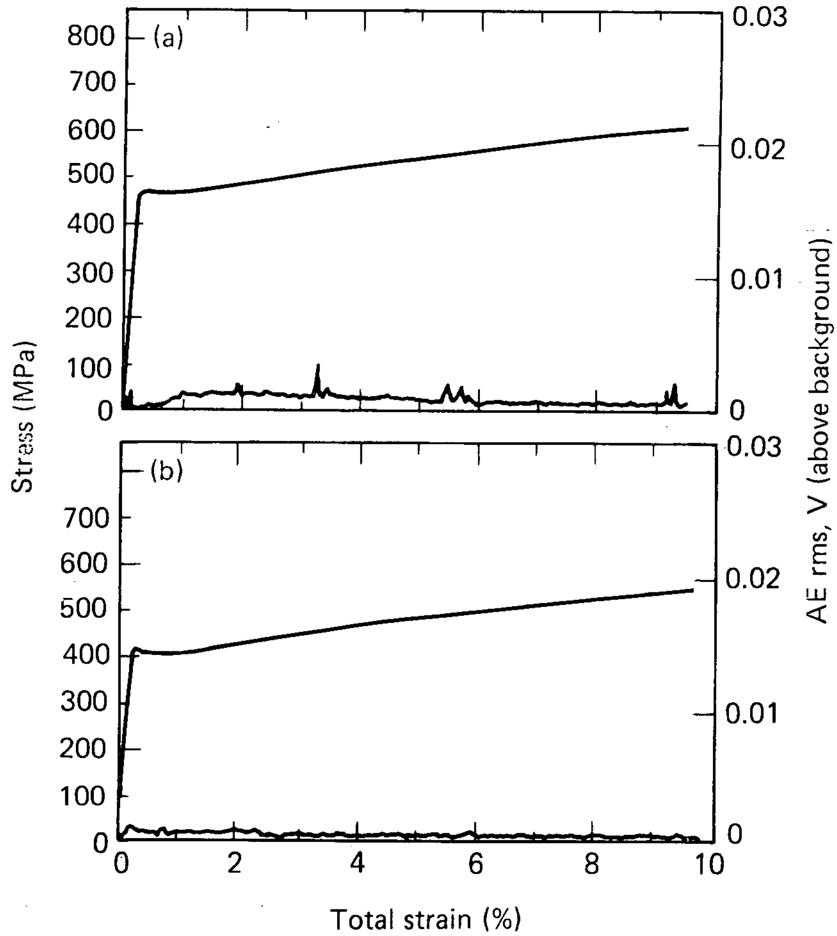

Fig. 11 - Hamstad

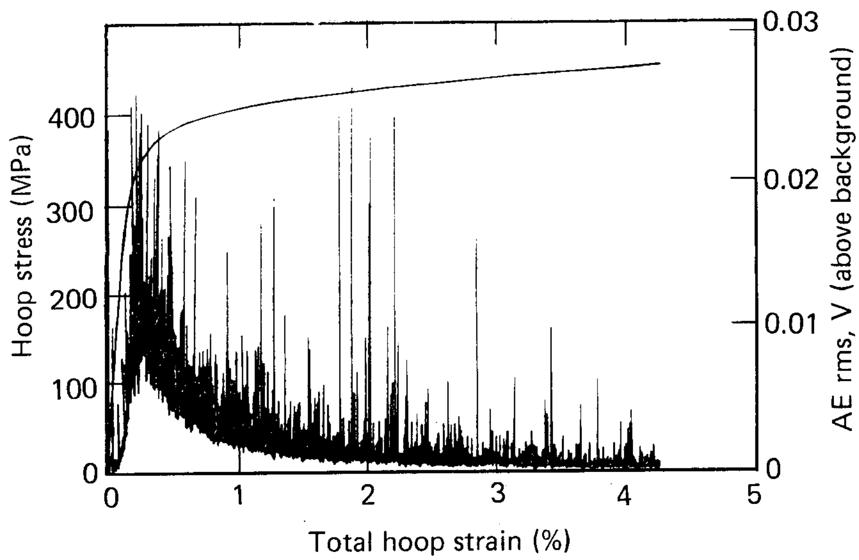

Fig. 12 - Hamstad

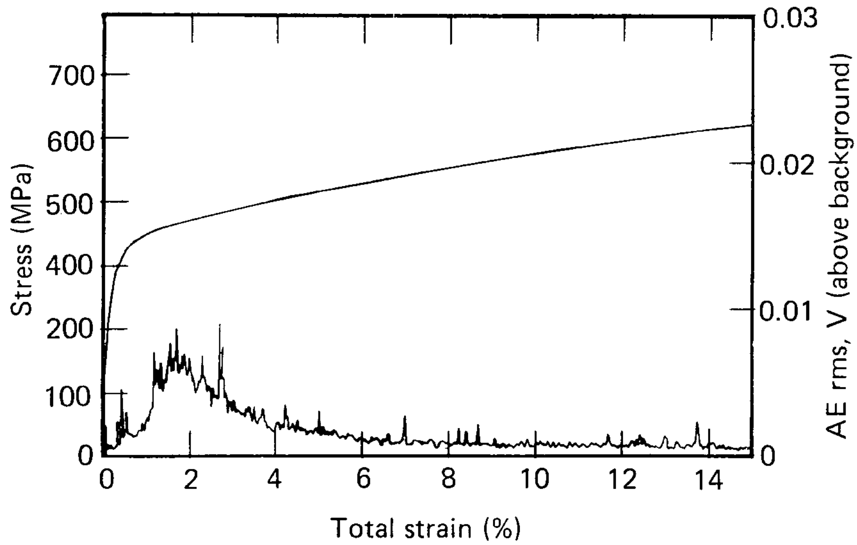

Fig. 13 - Hamstad

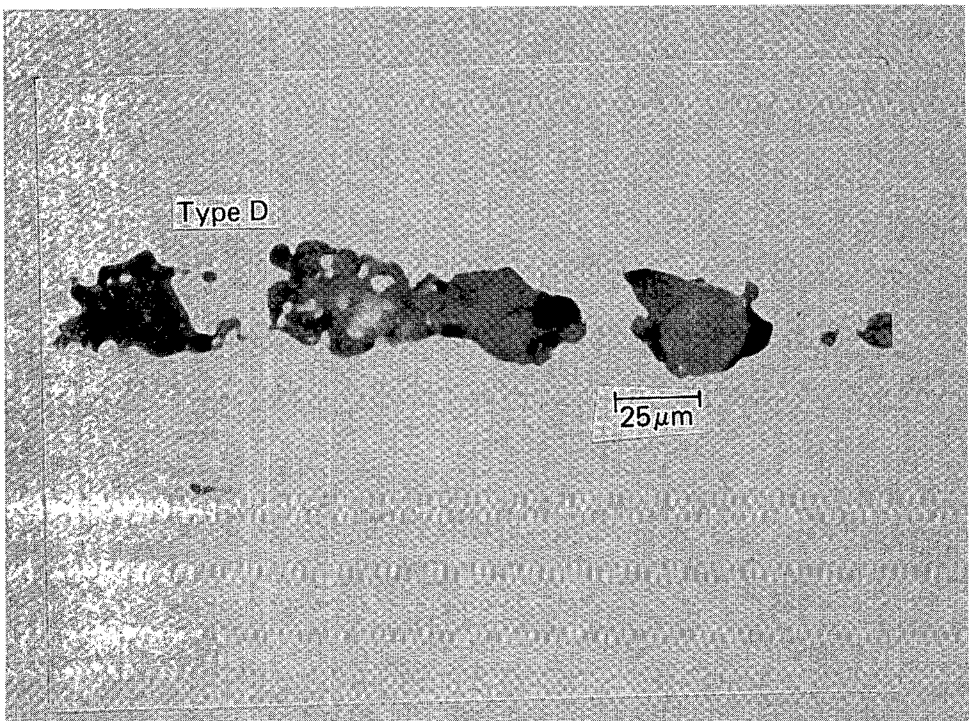

Fig. 14 - Hamstad

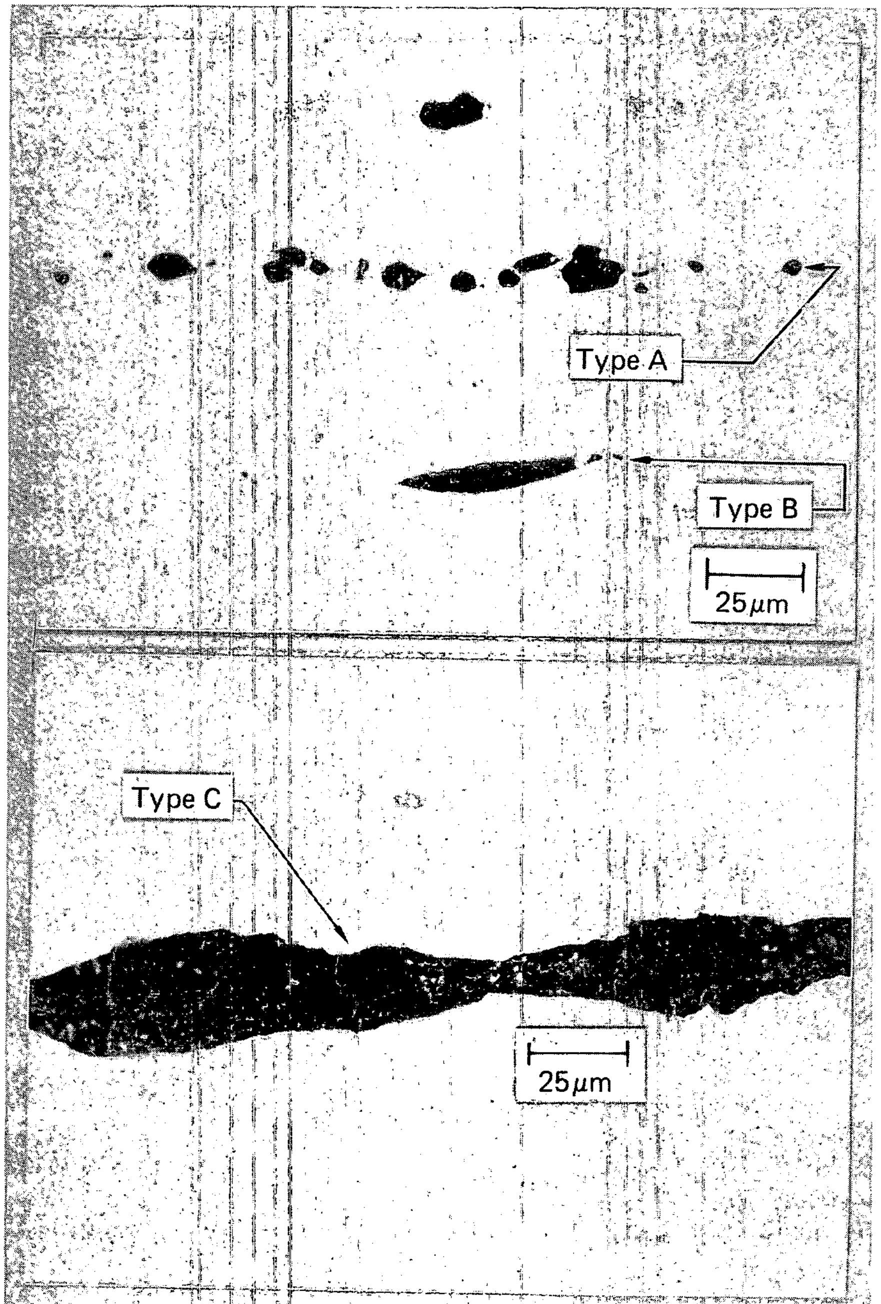

Fig. 15 - Hamstad

Technical Information Department · Lawrence Livermore Laboratory
University of California · Livermore, California 94550